Journal of Magnetics 8(4), 164-168 (2003)

A Computational Method to Consider the Saturation of Magnetic Field In a High Density Recording Head

Gwan Soo Park*

Dept. of Electrical and Computer Engineering, Pusan National University, Pusan 609-735, Korea

(Received 15 December 2003)

In high density recording system, the recording head field on a medium should be focused in small bit area and should have a sufficient value to overcome the medium coercivity, which resulted in head saturation. In this paper, an efficient method to access the head field and field gradient considering head saturation is presented. The magnetic vector potential on the head surface is pre-calculated considering head saturation in several cases and accumulated into database. The head field on the recording media is easily produced solving Laplace equation using accessed magnetic vector potential boundaries. The computed head field is compared with a quantified magnetic force microscopy measurement.

Key words : field gradient, magnetic recording head, head saturation, MFM measurement

1. Introduction

As the magnetic recording density approaches to 100 GB/in^2, new recording head designs are required. For high density recording, the head field should be high enough to overcome the media coercivity and be focused in a small bit area. Therefore, in the design of a recording head, not only the field value but field gradient is important for high density recording and the magnetic saturation of the head will be inevitable.

The main difficulty in the analyses of the magnetic head field is the scale problem. The dimension ratio of the head and the head gap is over one thousand. The recording region is around the head gap that has dimension of several hundred nanometers while the whole head has the dimension of millimeter. The effective field in recording is just on the media around the gap.

To achieve the high density in magnetic recording, the spacing between the head and the medium needs to be reduced. In this case, the recording region on the media is very close to the pole tip of the gap. Even in the case of a linear head, the conventional Karlqvist or conformal mapping type approximation shows disagreement with a finite element result as in Fig. 1 because of their assumptions. In the case we include the magnetic saturation of the recording head, a new efficient way to calculate head field considering head saturation is necessary.

In this paper, the new algorithm to generate head field considering head saturation is presented. The magnetic potentials on the head surface are calculated by a finite element method considering head saturation, and then accumulated on the database as boundary values. The head field on the medium is then calculated by Laplace equation with the boundary of the pre-accumulated database. The computed results are compared with magnetic force microscopy (MFM) quantification measurement in a real size head.

2. Boundary Potentials

The boundary potentials can be calculated by a conven-

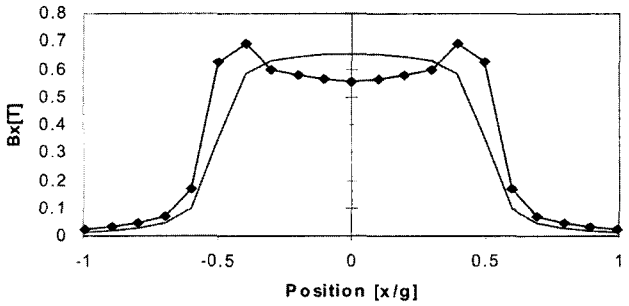

Fig. 1. X component of head field (gap: 1.0 μm, spacing: 500 Å) (Line: Karlqvist field, Dot: Finite element field)

*Corresponding author: Tel: +82-51-510-2788,
e-mail: gspark@pusan.ac.kr

tional finite element method concerning magnetic head saturation. There can be three methods to obtain boundary potentials on the head surface.

2.1. Scalar Potential method by Hx

In case of 2D, Maxwell equation shows the relation between magnetic flux density, vector potential and scalar potential as in (1).

$$B=\nabla\times A=-\mu_0\nabla\phi \tag{1}$$

$$H_x(y_0)=\frac{1}{\mu_0}\frac{\partial A}{\partial y}=-\frac{\partial\phi}{\partial x} \tag{2}$$

Fig. 2 shows the region of a recording medium and boundaries. In the case we set the boundary A to be $Hy=0$ and the boundary B to be $Hx=0$, the normal derivative of the scalar potential at the boundary will be zero, respectively. At the boundary C, the magnetic scalar potential can be obtained from the tangential component of magnetic field Hx as in (3).

$$\phi(y_0)=-\int H_x(y_0)dx \tag{3}$$

Fig. 3 shows the magnetic field intensity at the boundary C. Therefore, the scalar potential in the recording region can be calculated by Laplace equation as in (4).

$$\nabla^2\phi(x,\ y)=0 \tag{4}$$

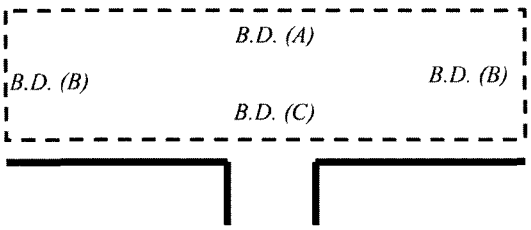

Fig. 2. Recording region and boundaries.

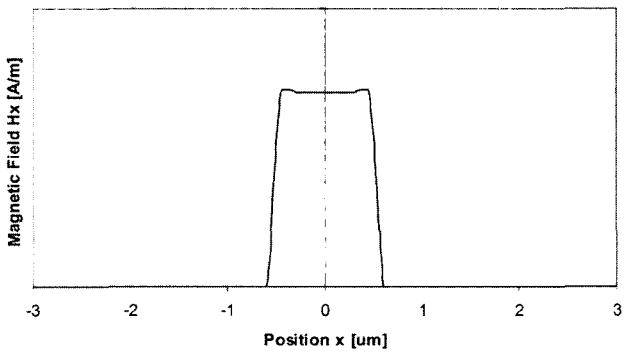

Fig. 3. Hx component on the boundary C in Fig. 2.

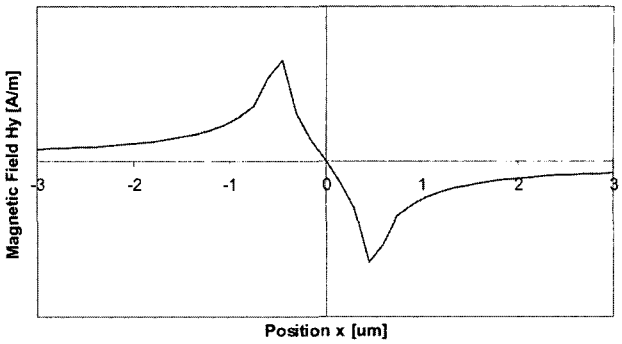

Fig. 4. Hy component on the boundary C in Fig. 2.

Magnetic field and field gradient can be calculated from the scalar potential as in (5).

$$Hx=-\frac{\partial\phi}{\partial x},\quad Hy=-\frac{\partial\phi}{\partial y} \tag{5}$$

As shown in Fig. 3, Hx on the head surface changes abruptly across the gap which prevents an accurate computation.

2.2. Scalar Potential method by Hy

The relation between the scalar potential and the normal component of the magnetic field intensity (Hy) could be expressed in (6). Therefore, the magnetic scalar potential can be obtained by (7).

$$H_y(y_0)=-\frac{1}{\mu_0}\frac{\partial A}{\partial x}=-\frac{\partial\phi}{\partial y} \tag{6}$$

$$\phi(y_0)=-\int H_y(y_0)dy \tag{7}$$

The boundary condition on the boundary A and B is equal to the previous case. The scalar potential in the recording region is calculated by (4) and magnetic field and field gradient can be calculated from the scalar potential as in (5).

Fig. 4 shows the magnetic field intensity at the boundary C. In the figure, Hy on the head surface is also changed abruptly across the gap which prevents the accurate computation.

2.3. Vector Potential method

The vector potential on the head surface is as in (8). This is the integration of the Hy in the direction of tangential component, the scalar potential on the boundary C is smooth as in Fig. 5. The magnetic field on the media can be therefore computed as in (9) and (10).

$$A(y_0)=-\mu_0\int H_y(y_0)dx \tag{8}$$

$$\nabla^2A(x,\ y)=0 \tag{9}$$

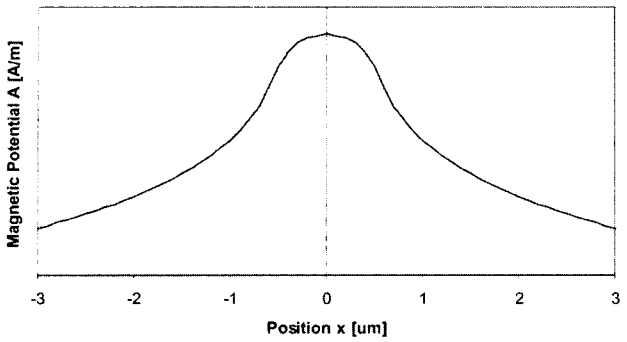

Fig. 5. Magnetic vector potential on the boundary C in Fig. 2.

$$Hx=-\frac{1}{\mu_0}\frac{\partial A}{\partial y},\quad Hy=\frac{1}{\mu_0}\frac{\partial A}{\partial x} \tag{10}$$

The magnetic vector potential is continuous between head material and air where magnetic field is discontinuous. Therefore, the magnetic vector potential boundary in the boundary C is directly defined on the head surface. But the magnetic field boundary should be defined in the air over the head surface that might cause error.

In the analyses, the sets of surface boundary values were pre-calculated by using the magnetic vector potential considering the head saturation and accumulated in the database.

3. Head Saturation

For the high density recording, the recording head field should be over 3 times of media coercivity and be focused in the small bit area. So, the magnetic saturation in the stitched pole type recording head is inevitable. During the recording simulation, there is nonlinear iteration for the hysteresis modeling of the recording media. If the magnetic saturation of the head is considered, there are so many iterations that the convergence of iteration is almost impossible. Therefore, the more simple way is necessary to access the head field when the head saturation is considered.

3.1. Saturation Factor

B-H curve of the head material can be simply defined by saturation factor S. Fig. 6 shows the typical B-H curve and the S factor is defined as in (11).

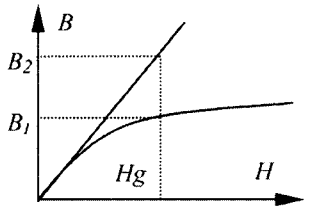

Fig. 6. Definition of head saturation factor S.

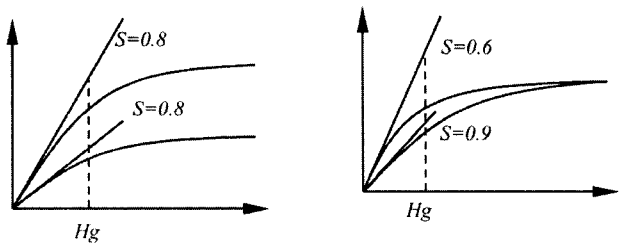

(a) Same S with different Bs (b) Different S with same Bs

Fig. 7. Two types of B-H curves and saturation factors.

$$S \equiv \left.\frac{B_2}{B_1}\right|_{H_g} \tag{11}$$

Hg in Fig. 6 is deep gap field. Head field on the medium is always less than deep gap field. If the head material is not saturated S is equal to one. In the case the head is saturated, S is bigger than one. So, the head saturation can be defined by S. In Fig. 7, there are two cases of the B-H curves. In Fig. 7(a), Bs of the two materials is different but S factor is the same. In this case, the head field patterns on the media are the same, so the normalized head field is the same. In other words, the head field distribution with the same S factor can be obtained from the same database.

In Fig. 7(b), although Bs of the two materials is the same, the S factor is different. In this case, the head field patterns on the media are different, so the normalized head field is also different. In other words, the head field distribution with different S factor should be obtained from different database.

3.2. Field Generator

The field distribution pattern is defined by S factor and gap, g. The magnetic vector potential boundary $Ao(x)$ at the surface of the recording head can be defined by three factors such as g, S, and Bs.

$$Ao(x) = Bs \times f(g, S) \tag{12}$$

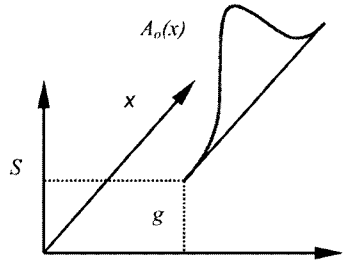

Fig. 8. Diagram of the potential boundary access in Fig. 2.

Then, $Ao(x)$ is pre-calculated in several cases. In this research, $g = 0.2$, 0.4, 0.6, 0.8, 1.0 micro meter and $S = 1.0$, 1.2, 1.4, 1.6, 1.8 cases are pre-calculated and accumulated in the database. So, if we need any field, we can access boundary $Ao(x)$ in boundary C in the Fig. 2 by adopting interpolation if necessary. Fig. 8 shows the diagram to access the $Ao(x)$. Magnetic potential on the media could be computed by solving Laplace equation as in (9), so does the magnetic field in (10).

4. Verification by MFM Measurement

The magnetic fields can be measured in real head size if the lateral field components can be neglected and point dipole approximation can be assumed in MFM tips. Trimmed MFM tip was made for this purpose. Fig. 9 shows the FIBE trimming tip that has 10 nm × 60 nm sized magnetic layer. Black region on the pole tip is a magnetic layer. Although this is not an ideal size to measure the point field, the MFM signal in this tip is mainly depended on the normal component of the pole tip. We developed quantification MFM measurement to measure high moment head field for the density 100 GB/in^2. Fig. 10 shows the MFM image of the ring head where the gap = 200 Å, spacing = 200 Å, width = 5 μm, thickness = 3.5 μm.

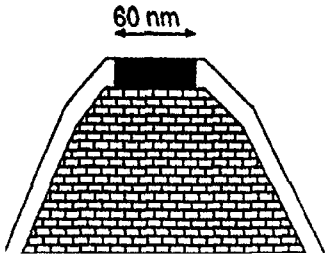

Fig. 9. MFM FIBE trimming tip for quantification measurement.

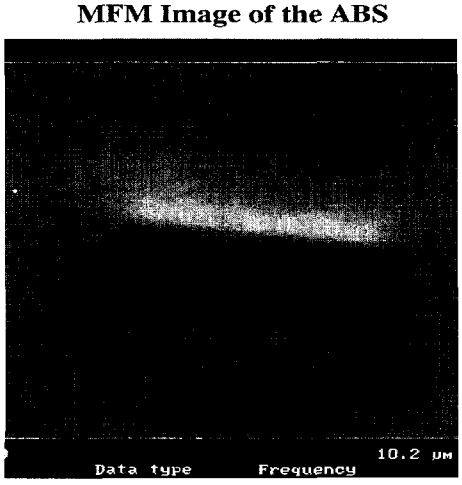

Fig. 10. MFM Image of the ABS (gap = 200 Å, spacing = 200 Å, width = 5 mm, thickness = 3.5 μm)

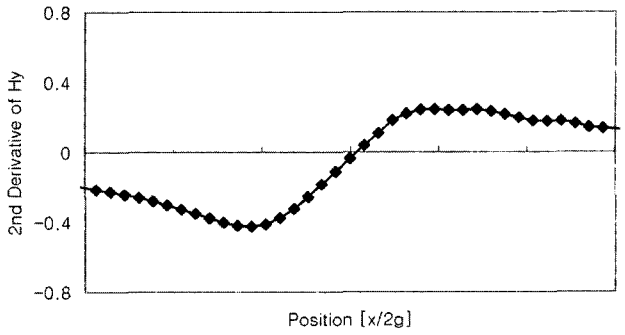

Fig. 11. Measured MFM signals.

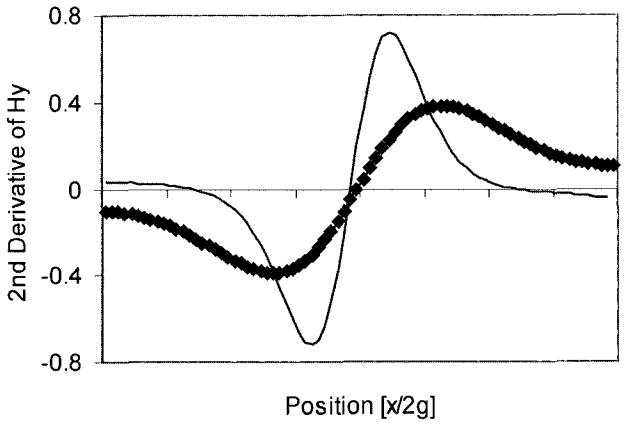

Fig. 12. Computed Results from vector potential method (dotted) and Karlqvist equation (line).

The MFM signal is proportional to the second derivative of the magnetic field if the magnetic moment on the MFM tip is assumed to be constant during the measurement as in (13).

$$Signal \approx M_y \cdot \frac{\partial^2 H}{\partial y^2} \tag{13}$$

Fig. 11 shows the measured MFM signal which is the second derivative of the head field. Signals are measured along the center of the head width across the gap and pole tip height is 200 Å from the head surface. In Fig. 12, computed result from the vector potential method and Karlqvist equation at the same position. The S factor in this computation is 1.17. Fig. 12 is the second derivative of the field and the maximum field is measured to be 192 kA/m. The measured MFM signal in Fig. 12 is agreed with the field computed by the method in this paper rather than the field computed by the Karlqvist equation. The result shows that the method in this paper gives a more realistic result because of the inclusion of magnetic

saturation of the recording head.

5. Conclusions

In this paper, the new method to generate magnetic head field considering head saturation is presented. In high density recording, the magnetic field and field gradient should be computed precisely for the analyses and design of the head. The magnetic potential method turns out to be better than magnetic scalar potential method. The magnetic vector potentials on the head surface is pre-calculated by a finite element method considering head saturation and accumulated in the database. The magnetic field and field gradient on a recording medium is computed solving Laplace equation using accessed magnetic vector potential boundaries. Quantitative MFM signals show agreement pattern with computed result but Karlqvist field is localized in the gap region too much.

References

[1] S. K. Khizroev, J. A. Bain, and M. H. Kryder, IEEE Trans. Magn. **33**(5), 2893 (1997).

[2] H. Neal Bertram, Theory of Magnetic Recording, Cambridge University Press, London (1994).

[3] H. L. Huang, T. Y. Lee, and Y. T. Huang, IEEE Trans. Magn. **28**(5), 2650 (1992).

[4] J. Fitzpatrick, and X. Che, IEEE Trans. Magn. **31**(3), 1095 (1995).